

DEVELOPMENT OF THE MANUFACTURING CAPABILITIES OF THE HYDROSTATIC EXTRUSION PROCESS

Volume I

**R. J. Fiorentino
B. D. Richardson
G. E. Meyer
A. M. Sabroff
F. W. Boulger**

**BATTELLE MEMORIAL INSTITUTE
COLUMBUS LABORATORIES**

**TECHNICAL REPORT AFML-TR-67-327, VOLUME I
October, 1967**

This document is subject to special export controls and each transmittal to foreign governments or foreign nationals may be made only with prior approval of the Manufacturing Technology Division of the Air Force Materials Laboratory, Wright-Patterson Air Force Base, Ohio 45433.



**METALLURGICAL PROCESSING BRANCH
MANUFACTURING TECHNOLOGY DIVISION
AIR FORCE MATERIALS LABORATORY
RESEARCH AND TECHNOLOGY DIVISION
AIR FORCE SYSTEMS COMMAND
WRIGHT-PATTERSON AIR FORCE BASE, OHIO**

FOREWORD

This final technical report in two volumes covers the work performed under Contract AF 33(615)-3190 from 1 December 1964 through 8 July 1967. Volume I covers the results of the experimental work in hydrostatic extrusion and Volume II contains the work relative to design and construction of high-pressure hydrostatic extrusion containers. The manuscript was released by the authors on 29 September 1967 for publication as an AFML technical report.

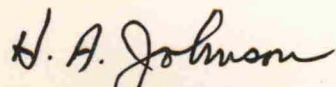
This contract with Battelle Memorial Institute of Columbus, Ohio, was initiated under Manufacturing Methods Project No. 8-198, "Development of the Manufacturing Capabilities of the Hydrostatic-Extrusion Process". It was administered under the technical direction of Mr. Charles S. Cook until September 1965 and then by Mr. Gerald A. Gegel of the Metallurgical Processing Branch (MATB), Manufacturing Technology Division, Air Force Materials Laboratory, Wright-Patterson Air Force Base, Ohio.

The program was conducted at Battelle with the prime responsibility assigned to the Metalworking Research Division and with Mr. R. J. Fiorentino, Associate Chief, as Project Engineer. Others contributing to the program were Mr. B. D. Richardson, Research Metallurgical Engineer, Mr. G. E. Meyer, Research Metallurgical Engineer, Mr. F. W. Fawn, Technician, Mr. A. M. Sabroff, Division Chief, and Mr. F. W. Boulger, Senior Technical Advisor. The late Mr. W. R. Hansen, Research Metallurgist, made a significant contribution to the program up to the time of his death in August, 1966. Mr. R. L. Jentgen, Associate Chief in the Structural Physics Division, assisted in the fluid and lubrication studies of the program. Dr. J. C. Gerdeen, Senior Research Mechanical Engineer in the Advanced Solid Mechanics Division, conducted the stress analysis for the high-pressure-container-design study. Mr. E. C. Rodabaugh, Mr. M. Vagins, Senior Mechanical Engineers, and Mr. T. J. Atterbury, Chief of the Applied Solid Mechanics Division, also assisted in this study. Mr. R. E. Mesloh, Research Mechanical Engineer of the Applied Solid Mechanics Division, designed an instrument for measuring fluid pressure at elevated temperatures. Data from which this report has been prepared are contained in Battelle Laboratory Record Books Nos. 21799, 21990, 23065, 23287, 23585, 23791, 23836, and 24446.

This project has been accomplished as a part of the Air Force Manufacturing Methods program, the primary object of which is to develop, on a timely basis, manufacturing processes, techniques, and equipment for use in economical production of USAF materials and components. The program encompasses the following technical areas:

- Metallurgy - Rolling, Forging, Extruding, Casting, Fiber, Powder.
- Chemical - Propellant, Coating, Ceramic, Graphite, Nonmetallics.
- Fabrication - Forming, Material Removal, Joining, Components.
- Electronics - Solid State, Materials and Special Techniques, Thermionics.

Suggestions concerning additional Manufacturing Methods development required on this or other subjects will be appreciated.



H. A. JOHNSON, Chief
Metallurgical Processing Branch
Manufacturing Technology Division

ABSTRACT

The purpose of the program was to develop the manufacturing capabilities of the hydrostatic-extrusion process. Specific applications studied were fabrication of wire, tubing, and shapes from relatively difficult-to-work materials such as refractory-metal alloys, high-strength steels, aluminum alloys, titanium alloys, beryllium, and other selected materials. Phase I was concerned with process optimization and Phase II with direct process application.

As part of Phase I, the effects of critical process variables on pressure requirements and product quality were studied for wrought and powder materials ranging from relatively high-strength easy to work materials such as aluminum alloys and steels to the relatively more difficult-to-work materials such as Ti-6Al-4V titanium alloy and superalloys. With these materials, fluids and lubricants tended to be the factor controlling pressure requirements and product quality. With almost every material extruded the limit in extrusion ratio was set by the design pressure capacity of the container except for the aluminum alloys where the limit was set more by the efficiency of the lubrication system.

In the hydrostatic extrusion of brittle materials, die design proved to be the most significant factor controlling the production of sound, good quality extrusions. New die-design concepts have opened up new fields for the application of hydrostatic extrusion to brittle materials.

Except for the aluminum alloys, the hydrostatic extrudability of the above range of materials was also investigated at 400 and 500 F. Again, fluids and lubricants were developed to enable the production of good quality extrusions. Of particular interest here was the wide range of lubricants that operated successfully at this temperature level.

As part of Phase II of the program, tubing, mill shapes and wire were produced from a variety of materials. For tubing, the floating-mandrel arrangement enabled higher extrusion-ratio capabilities than those for solid rounds. An analysis of the beneficial effects of the floating-mandrel arrangement is given.

T-sections were extruded from round billets and were re-extruded into smaller T-sections. Materials evaluated here were 7075-0 aluminum, AISI 4340 steel, Ti-6Al-4V alloy and Cb752 columbium alloy. The problem of sealing against leaks between the T-billet and die in the re-extrusion of shapes was overcome to some extent following the evaluation of several methods of sealing.

In the reduction of T-sections and wire, a technique of hydrostatic-extrusion drawing developed at Battelle was used. This method, called the HYDRAW technique, was used to reduce wire of Ti-6Al-4V alloy, beryllium, and TZM molybdenum alloy wire at single pass reductions of up to 60 percent. That reduction appeared to be by no means the limit of single-pass reduction achievable with these materials.

During the experimental program, a study of high-pressure container designs was made. Several design concepts that were analyzed are presented in detail in this report. The most promising concept for containing fluid pressures up to 450,000 psi in large-bore containers was that of using pressurized-fluid support as in the ring-fluid-ring design. This and other designs were analyzed on the basis of fatigue-strength criterion, which is believed to be a new and more sound basis for the design of high-pressure containers.

This document is subject to special export controls and each transmittal to foreign governments or foreign nationals may be made only with prior approval of the Manufacturing Technology Division

TABLE OF CONTENTS

	<u>Page</u>
I. INTRODUCTION	1
II. SUMMARY VOLUME I	3
III. EQUIPMENT AND PROCEDURE	8
Extrusion Tooling	8
The Hydrostatic Extrusion Operational Sequence	8
Pressure Control and Measurement	11
High-Pressure Strain-Gage Transducer	11
Sealing Arrangements	15
Room Temperature	15
Temperature Range of 400-500 F	16
Die Design	17
Billet Materials	19
Lubrication	19
Hydrostatic Fluids	22
Billet Lubricants	22
Billet Conversion Coatings	24
IV. CHARACTERISTICS OF PRESSURE-DISPLACEMENT CURVES	26
V. ASSESSMENT OF FLUID HEATING EFFECTS DURING COMPRESSION	28
SECTION I	
VI. SUMMARY SECTION I	31
VII. COLD HYDROSTATIC EXTRUSION OF 7075-0 ALUMINUM ROUNDS	36
Extrusion Ratio	36
Reliability of Data	38
Billet Finish	38
Lubrication Systems	38
Billet Nose Design	41
Stem Speed	43
Tensile Properties of 7075-0 Aluminum Hydrostatic Extrusions	46
VIII. HYDROSTATIC EXTRUSION OF AISI 4340 STEEL ROUNDS	47
Extrusion Ratio	47
Fluids and Billet Lubrication at 80 F	53
Billet Lubricants and Coatings	54
Hydrostatic Fluids	57
Billet Surface Finish	58

TABLE OF CONTENTS
(Continued)

	<u>Page</u>
Stem Speed	58
Hydrostatic Extrusion of AISI 4340 Steel at	
Elevated Temperatures	60
Extrusion at 140 F	60
Extrusion at 400 and 500 F	61
Tensile Properties of AISI 4340 Steel Hydrostatic Extrusions	63
 IX. HYDROSTATIC EXTRUSION OF Ti-6Al-4V TITANIUM	
ALLOY ROUNDS	65
Extrusion Ratio	65
Lubrication at 80 F	65
Evaluation of Billet Lubricants Without Billet Coatings	65
Evaluation of Billet Lubricants and Billet Coatings	70
Fluids at Room and Elevated Temperatures	72
Billet Lubricants at 400 and 500 F	72
Effect of Temperature	73
Mechanical Properties of Ti-6Al-4V Titanium Alloy Rounds	
Produced by Cold Hydrostatic Extrusion	73
 X. HYDROSTATIC COMPACTION AND HYDROSTATIC EXTRUSION OF	
POWDER COMPACTS OF Ti-6Al-4V ALLOY POWDER	74
Hydrostatic Compaction of Ti-6Al-4V Titanium Alloy Powder	74
Hydrostatic Extrusion of Powder Compacts of Ti-6Al-4V	
Alloy Powder	75
 XI. HYDROSTATIC EXTRUSION OF SUPERALLOYS ALLOY 718 AND A286	76
Tensile Properties of Hydrostatic Extrusions of Alloy 718 and	
A-286 Superalloys	76
 XII. COLD HYDROSTATIC EXTRUSION OF DISPERSION-HARDENED	
SINTERED ALUMINUM	78
 XIII. HYDROSTATIC EXTRUSION OF BRITTLE MATERIALS	80
Extrusion Ratio	80
Die Designs	84
Effect of Die Design, Extrusion Ratio, and Temperature	
on TZM	86
Evaluation of Die Designs at an Extrusion Ratio of 2.5:1	86
Controlled-Relief Die - Extrusion Ratio 3.3:1	86
Standard Die - Extrusion Ratio 5:1	86
Double-Reduction Die - Extrusion Ratio 4:1	88
Effect of Die Design, Extrusion Ratio, and Temperature	
on Beryllium	89

TABLE OF CONTENTS

(Continued)

	<u>Page</u>
Controlled-Relief Die	89
Double-Reduction Die - Extrusion Ratio 4:1	89
The Potential of Die Design	93
SECTION II	
XIV. SUMMARY OF SECTION II	97
XV. HYDROSTATIC EXTRUSION OF TUBING	98
Tooling	98
Effect of Floating-Mandrel Arrangement	98
7075-O Aluminum Tubing	102
Extrusion Ratio	102
Lubrication	102
Effect of Stem Speed	104
Extrusion Ratio	104
Lubrication	104
Effect of Mandrel Taper	106
Re-Extrusion of As-Extruded Tubing	106
Ti-6Al-4V Titanium Alloy Tubing	106
Extrusion Ratio	107
Effect of Mandrel Taper	107
Lubrication	107
Stem Speed	109
Re-Extrusion of As-Extruded Tube	109
XVI. HYDROSTATIC EXTRUSION OF SHAPES	110
Die Design for the Extrusion of Shapes	110
Die Design for the Extrusion of Shapes From	
Round Billets	110
Die Design for Re-extrusion of T-Sections	110
Experimental Procedure	113
Cold Hydrostatic Extrusion and Re-extrusion of 7075-0	
Aluminum Shapes	113
Extrusion Pressure Requirements	113
Die Design	115
Stem Speed and Billet Surface Finish	115
Billet Lubrication	115
Extrusion of Re-entrant Channel Section	115
Re-extrusion of 7075-0 Al T-Sections	115
AISI 4340 Steel T-Sections	116
Re-extrusion of Ti-6Al-4V Alloy T-Sections	118
Re-extrusion of Cb-752 Columbium Alloy T-Section	118

TABLE OF CONTENTS (Continued)

	<u>Page</u>
XVII. THE HYDRAW OF WIRE AND SHAPES	120
The HYDRAW Process	120
HYDRAW Tooling	120
Draw Control and Draw Load Measurement	120
Wire Coil Configurations	122
Experimental HYDRAW Procedure	122
Preparation of the Point on Wire and Shape	122
Operational Sequence	124
HYDRAW of Ti-6Al-4V Titanium Alloy Wire	124
HYDRAW of Beryllium Wire	126
The Starting Wire	128
Experimental Developments	128
HYDRAW of Beryllium Wire of Ingot Origin	130
HYDRAW of Beryllium Wire of Powder Metallurgy Origin	131
Tensile Data on Beryllium Wire	131
HYDRAW of TZM Molybdenum Alloy Wire	132
HYDRAW of 7075-0 Aluminum T-Sections	132
XVIII. TANDEM EXTRUSION	134
XIX. ECONOMIC ANALYSIS OF THE HYDROSTATIC EXTRUSION OF SOLID ROUNDS AND TUBING	137
Conversion Costs to Produce Rounds by Hydrostatic Extrusion and by Conventional Hot Extrusion	139
Hydrostatic Extrusion of Rounds	139
Conventional Hot Extrusion	141
Comparison of Hydrostatic Extrusion and Hot Extrusion Conversion Costs	141
Conversion Costs to Produce Ti-6Al-4V Titanium Alloy Tubing by Hydrostatic Extrusion	142
XX. REFERENCES	147

LIST OF ILLUSTRATIONS

<u>Figure</u>		<u>Page</u>
1.	Hydrostatic Extrusions of Aluminum Alloys	5
2.	Hydrostatic Extrusions of High Strength and Brittle Materials	5
3.	Hydrostatically Extruded Tubing From Three Alloys	7
4.	Hydrostatic-Extrusion Tooling Installed in 700-Ton Vertical Hydraulic Press at Battelle	9
5.	Assembly Drawing of Tooling for Hydrostatic Extrusion	10
6.	Details of Hydrostatic Extrusion Process Showing the Stem and Die Seal Methods, and Partially Extruded Billet	12
7.	Temperature Resistivity Curve for Manganin Wire	13
8.	High-Pressure Transducer Developed at Battelle for Measuring High Fluid Pressures at Room and Elevated Temperatures	14
9.	Die Seal Arrangements Evaluated in Hydrostatic Extrusion	16
10.	Stem-Seal Arrangement Used for Warm Hydrostatic Extrusion	17
11.	Die Design With Helical Groove in Conical-Entry Surface	18
12.	Relationship Between Extrusion Pressure, Extrusion Ratio, and Billet Hardness	34
13.	Effect of Extrusion Ratio on Fluid Runout Pressures in the Hydrostatic Extrusion of 7075-O Aluminum Rounds	37
14.	Effect of Fluid and Billet Lubricant on Pressure-Displacement Curves Obtained in the Hydrostatic Extrusion of 7075-O Aluminum at a Ratio of 20:1	42
15.	Two Billet Nose Designs Evaluated in Hydrostatic Extrusion	44
16.	Effect of Billet Nose Shape on Pressure-Displacement Curves Obtained in the Hydrostatic Extrusion of 7075-O Aluminum at a Ratio of 40:1	45
17.	Effect of Extrusion Ratio on Pressures Required for Hydrostatic Extrusion of AISI 4340 Steel	52
18.	Effect of Stem Speed on Fluid Pressures for Cold Hydrostatic Extrusion of AISI 4340 at an Extrusion Ratio of 5:1	59
19.	Effect of Extrusion Ratio on Runout-Fluid Pressures for Ti-6Al-4V Rounds	69

LIST OF ILLUSTRATIONS
(Continued)

<u>Figure</u>		<u>Page</u>
20.	Comparison of Surface Finishes on Cold Hydrostatic Extrusions of Ti-6Al-4V Made at a Ratio of 3.33:1	71
21.	Influence of Extrusion Ratio on Pressures for Beryllium and Wrought TZM	83
22.	Standard Die Profile and Two Dies Designed to Eliminate Cracking in Brittle Materials	85
23.	Influence of Double-Reduction Die on Cracking of Hydrostatic Extrusions of Wrought TZM Molybdenum Alloy	87
24.	Influence of Die Design on Cracking in Hydrostatic Extrusions of Beryllium	90
25.	Photomicrographs of Beryllium Cold Hydrostatically Extruded at a Ratio of 4:1 Through Battelle's Double-Reduction Die	92
26.	Classification of Pressure-Displacement Curves Obtained in Hydrostatic Extrusion	95
27.	Floating Mandrel Arrangement for Hydrostatic Extrusion of Tubing	99
28.	Effect of Extrusion Ratio on Pressure for Cold Hydrostatic Extrusion of 7075-O Aluminum Tubing and Rounds	103
29.	Effect of Extrusion Ratio on Pressure for Cold Hydrostatic Extrusion of AISI 4340 Tubing and Rounds	105
30.	Effect of Extrusion Ratio on Pressure for Cold Hydrostatic Extrusion of Ti-6Al-4V Tubing and Rounds	108
31.	Two Die Designs Used in the Hydrostatic Extrusion of T-Sections From Round Billets	111
32.	Die Insert and Orifice Dimensions for a Re-Entrant Channel Section	112
33.	Die Design for Hydrostatic Extrusion of T-Section Billets	112
34.	T-Sections Produced by HYDRAW and Re-Extrusion	119
35.	Tooling Set-Up for HYDRAW of Wire	121
36.	Two Methods of Unreeling Wire From Within a Small-Bore Container	123
37.	Counterbored Tandem Billet Joint Design Evaluated in Hydrostatic Extrusion	134
38.	Tapered Tandem Billet Joint Design Evaluated in Hydrostatic Extrusion	134

LIST OF TABLES

<u>Table</u>		<u>Page</u>
I	Billet Materials Used in Hydrostatic Extrusion Program	20
II	Fluids Evaluated in Hydrostatic-Extrusion Program	22
III	Billet Lubricants Evaluated in Hydrostatic Extrusion Program	23
IV	Billet Conversion Coatings Evaluated in the Hydrostatic-Extrusion Program	25
V	Empirical Equations Relating Pressure and Extrusion Ratio for Cold Hydrostatic Extrusion of Several Materials	32
VI	Experimental Data for 80 F Hydrostatic Extrusion of 7075-O Aluminum Rounds at a Ratio of 20:1 and Stem Speed of 20 IPM	39
VII	Additional Experimental Data for 80 F Hydrostatic Extrusion of 7075-O Rounds	40
VIII	Room-Temperature Tensile Properties of 7075 Aluminum Rounds Produced by Hydrostatic Extrusion	46
IX	Investigation of Lubrication Systems Under Constant Extrusion Conditions for 80 F Hydrostatic Extrusion of AISI 4340 Rounds	48
X	Investigation of Extrusion Ratio, Stem Speed, and Die Angle for 80 F Hydrostatic Extrusion of AISI 4340 Rounds	50
XI	Experimental Data for Hydrostatic Extrusion of AISI 4340 Rounds at Elevated Temperatures	51
XII	Effect of Billet Lubrication in Hydrostatic Extrusion of AISI 4340 With Castor Oil as the Fluid Medium	55
XIII	Effect of Fluid Medium and Billet Lubrication in Hydrostatic Extrusion of AISI 4340 at 80 F	56
XIV	Effect of Die Angle on Extrusion Pressures at Two Ratios	59
XV	Comparison of Pressures Obtained in the Hydrostatic Extrusion of AISI 4340 Steel at 80, 120, and 140 F	60
XVI	Effect of Fluid on Pressures for Warm Hydrostatic Extrusion of AISI 4340 Steel	62
XVII	Evaluation of Lubricants Used in Extruding AISI 4340 Steel at 500 F	63
XVIII	Room-Temperature Tensile Properties of AISI 4340 Steel Rounds Produced by Hydrostatic Extrusion	64

LIST OF TABLES
(Continued)

<u>Table</u>	<u>Page</u>
XIX Experimental Data for 80 F Hydrostatic Extrusion of Ti-6Al-4V Rounds	66
XX Experimental Data for Hydrostatic Extrusion of Ti-6Al-4V Rounds at 400 and 500 F	68
XXI Tensile Properties of Ti-6Al-4V Alloy Rounds Produced by Hydrostatic Extrusion	73
XXII Experimental Data for Hydrostatic Extrusion of Superalloys	76
XXIII Tensile Properties and Hardness of Hydrostatic Extrusions Made From Superalloys A-286 and Alloy 718	77
XXIV Experimental Data for Cold Hydrostatic Extrusion of Dispersion-Hardened Sintered Aluminum	78
XXV Mechanical Properties of Sintered-Aluminum Product as Worked by Cold Hydrostatic Extrusion and Hot Conventional Extrusion	79
XXVI Experimental Data for Hydrostatic Extrusion of TZM Rounds at 80 and 500 F	81
XXVII Experimental Data for Hydrostatic Extrusion of Beryllium Rounds at 80 and 500 F	82
XXVIII Tensile Properties of Beryllium Hydrostatically Extruded Cold at an Extrusion Ratio of 4:1	94
XXIX Experimental Data for 80 F Hydrostatic Extrusion of Tubing From 7075-O Al, AISI 4340, and Ti-6Al-4V	100
XXX Experimental Data for 80 F Hydrostatic Extrusion and Re-Extrusion of 7075-O Aluminum T-Sections	114
XXXI Experimental Data for 80 F Hydrostatic Extrusion and Re-Extrusion of T-Sections of AISI 4340, Ti-6Al-4V, and Cb 752 Columbium Alloy	117
XXXII Experimental Data for HYDRAW of Ti-6Al-4V Wire at 80 and 500 F	125
XXXIII Selected Experimental Data for HYDRAW of Beryllium Wire	127
XXXIV Average Tensile Properties of Beryllium Wire Before and After Hydrostatic Extrusion Drawing at 500 F	131

LIST OF TABLES
(Continued)

<u>Table</u>	<u>Page</u>
XXXV Experimental Data Obtained in the Investigation of Tandem Extrusion at 80 F	135
XXXVI The Economic Basis for Determining Press Costs	138
XXXVII Billet Weights for Hydrostatic Extrusion and Hot Extrusion as a Function of Billet Material	140
XXXVIII Conversion Costs Per Pound of Extrusion for Hydrostatic Extrusion and Hot Extrusion as a Function of Die Life and a Variety of Materials	140
XXXIX Estimated Conversion Costs for Producing Ti-6Al-4V Titanium Alloy Tubing by Hydrostatic Extrusion Techniques	144
XL Estimated Conversion Costs for Producing Titanium and Ti-6Al-4V Tubing by Conventional Techniques	145

INTRODUCTION

The purpose of this program was to develop the manufacturing capabilities of the hydrostatic extrusion process and was divided into two phases with the following general objectives:

Phase I. Process-Development Studies

- Part 1. (a) To study the effect of critical process variables on pressure requirements and surface quality in hydrostatic extrusion of AISI 4340 steel, Ti-6Al-4V titanium alloy, and 7075 aluminum alloy.

(b) To correlate all available hydrostatic-extrusion-pressure data with material properties wherever possible in order to assist direction of the experimental effort and maximize the information developed on the present program.
- Part 2. To explore the hydrostatic extrudability of TZM molybdenum alloy, beryllium, A286 iron-base superalloy, Alloy 718 nickel-base superalloy, powder compacts, and other selected materials.
- Part 3. To conduct a design study for high-temperature, high-pressure hydrostatic-extrusion tooling based on (1) estimated pressure requirements for high-ratio extrusion of materials of interest to the Air Force, (2) latest high-pressure-vessel technology, and (3) latest tooling materials available.
- Part 4. To conduct a process economic study on the construction, installation, and operation of equipment with the same operational and size requirements as the tooling developed in the previous program on Contract No. AF 33(600)-43328.

Phase II. Process-Application Studies

- Part 1. To evaluate the application of the hydrostatic-extrusion process for sizing and finishing conventionally hot-extruded (or rolled) structural shapes by various combinations of drawing and extruding. Primary emphasis was to be on AISI 4340 steel, although some effort was to be devoted to Ti-6Al-4V, 7075-0 aluminum, and selected refractory metals.

Part 2. To determine the feasibility of producing wire and filaments from beryllium, TZM molybdenum alloy, and Ti-6Al-4V titanium alloy by combinations of hydrostatic extrusion and drawing.

Part 3. To develop tooling and define process parameters necessary for the reduction of tube blanks to finished tubing from AISI 4340 steel, 7075-0 aluminum, and Ti-6Al-4V titanium.

The results of the experimental and analytical work connected with Phases I and II were covered in Interim Engineering Progress Reports I through IX.

This, the Final Technical Report in two volumes, contains the results of the program in their entirety. Volume I contains Section 1, "A Study of the Critical Process Variables in the Hydrostatic Extrusion of Several Materials" and Section 2, "Production Aspects of Hydrostatic Extrusion". Volume II contains Section 3, "Analysis of Several High-Pressure Container-Design Concepts" and Section 4, "Hydrostatic-Extrusion Containers Designed and Constructed in the Program". The experimental program started December 1, 1964, and was completed on July 8, 1967.

II

SUMMARY VOLUME I

The experimental work conducted in this program has taken the technology of the hydrostatic-extrusion process from the experimental stage to the threshold of its application in a production operation. Commercial exploitation of the process is possible without any further major experimentation and it is believed that this report gives the guidelines which will enable these steps to be taken immediately. What remains now is the complete design of production hydrostatic-extrusion equipment. At the time of this writing, a program is underway at Battelle-Columbus Laboratories in which such equipment is being designed. The program, "Design Study of Production Press for Ultrahigh-pressure Hydrostatic Extrusion Equipment", is sponsored by the Metallurgical Processing Branch, Manufacturing Technology Division at Wright-Patterson Air Force Base, Ohio, on Contract No. F33(615)-67-C-1434.

This report describes the steps which were taken to firmly establish the production potential of hydrostatic extrusion. It was convenient to divide the report into four distinct sections, each covering a specific area of work:

Volume I

Section 1. A Study of the Critical Process Variables in the Hydrostatic Extrusion of Several Materials.

Section 2. Production Aspects of Hydrostatic Extrusion.

Volume II

Section 3. Analysis of Several High-Pressure-Container Design Concepts.

Section 4. Hydrostatic-Extrusion Containers Designed and Constructed in the Program.

These sections are complete in themselves and contain their own summaries. However, it is possible to summarize the results more generally at this point to give an overall picture of the achievements. Major accomplishments obtained in Sections I and II of the program are given below:

- (1) Beryllium was cold extruded into a 7/8-inch-diameter round at a ratio of 4:1 virtually free of cracks. This is an extremely significant advancement in the cold working of beryllium, particularly since it was achieved using Battelle's double-reduction die and without the need of an expensive, fluid counter-pressure system.

Another brittle material, TZM molybdenum alloy, was also cold extruded at 4:1 without cracks, using the double-reduction die.

- (2) Several samples of 0.020-inch diameter, beryllium wire originating from both ingot and powder material were hydrostatically extrusion-drawn to 0.0124 inch diameter (a reduction of 60 percent) at 500 F.

Two other wire materials, Ti-6Al-4V alloy and TZM molybdenum alloy were cold hydrostatic extrusion-drawn at reductions of up to 60 percent.

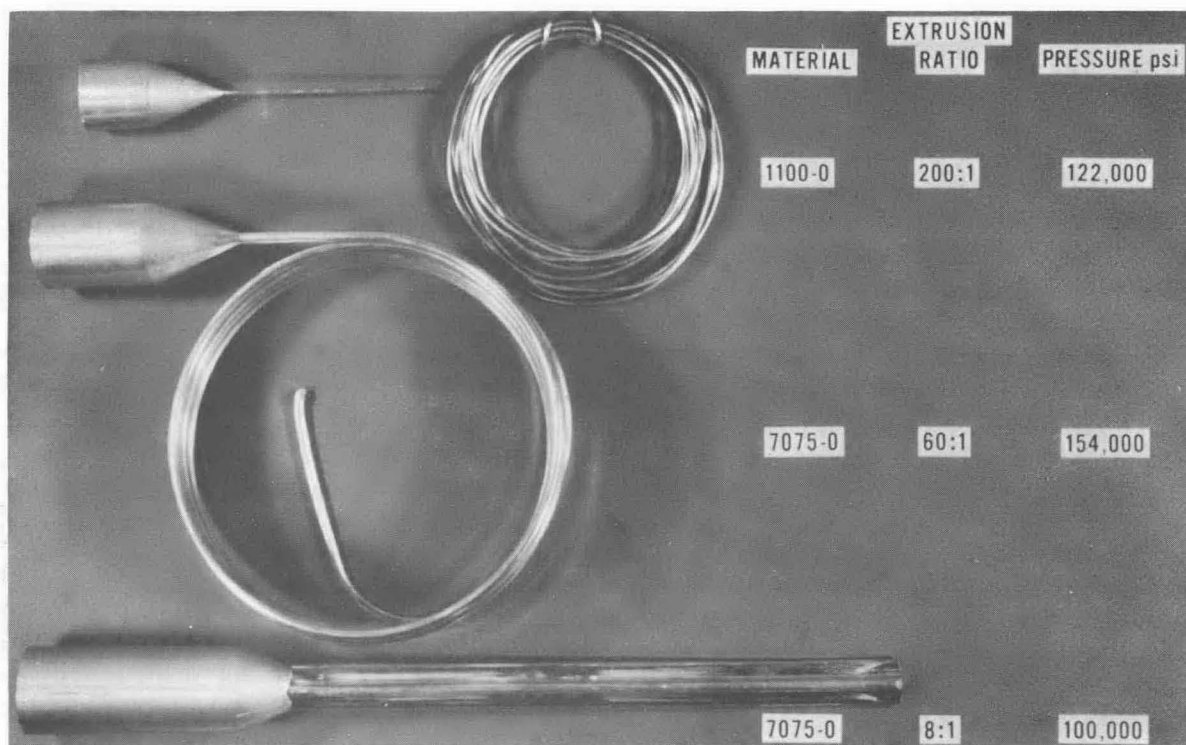
- (3) High-quality thin-walled Ti-6Al-4V tubing, 0.663-inch OD and 0.030-inch wall, was produced in a single-pass reduction of 60 percent at room temperature.

Good-quality thin-walled tubing was also produced by re-extruding previously hydrostatically extruded tubing.

- (a) With AISI 4340 steel, the cumulative reduction was 91 percent.
- (b) With 7075-0 aluminum, the cumulative reduction was 98 percent.
- (4) A selection of fluids and billet lubricants have been developed which provide optimum pressure levels and good finishes for a variety of materials at temperatures up to 500 F.
- (5) With most materials evaluated, extrusion at 500 F resulted in marked reductions in pressure requirements. Few problems in lubrication occurred at this temperature level.
- (6) Two superalloys, A286 and Alloy 718, were cold extruded without cracking through a die of standard design. The maximum extrusion ratios achievable within the 250,000 psi pressure capacity of the tooling were 5:1 and 3.3:1, respectively.
- (7) Tandem extrusion (of two billets in sequence) of 7075-0 aluminum billets with a counterbored joint was achieved without separation or any discontinuity in the extrusion pressures.
- (8) 7075-0 aluminum was cold extended at ratios up to 60:1 and exit speeds up to 250 fpm without surface cracking.
- (9) In the extrusion of T-sections from round billets, a compound-angle entry orifice was found to provide minimum pressure requirements.
- (10) Tensile test data obtained on hydrostatic extrusions of all materials indicated significant increases in strength over that in the billet material with good retention of ductility.

Beryllium wire was markedly strengthened by the area reductions indicated in Item (2). Its ductility (as measured by elongation) was reduced from 2.5 percent to less than 1 percent, but remained sufficiently high to withstand the application of a draw stress and coiling around a 3-inch-diameter reel without breakage occurring.

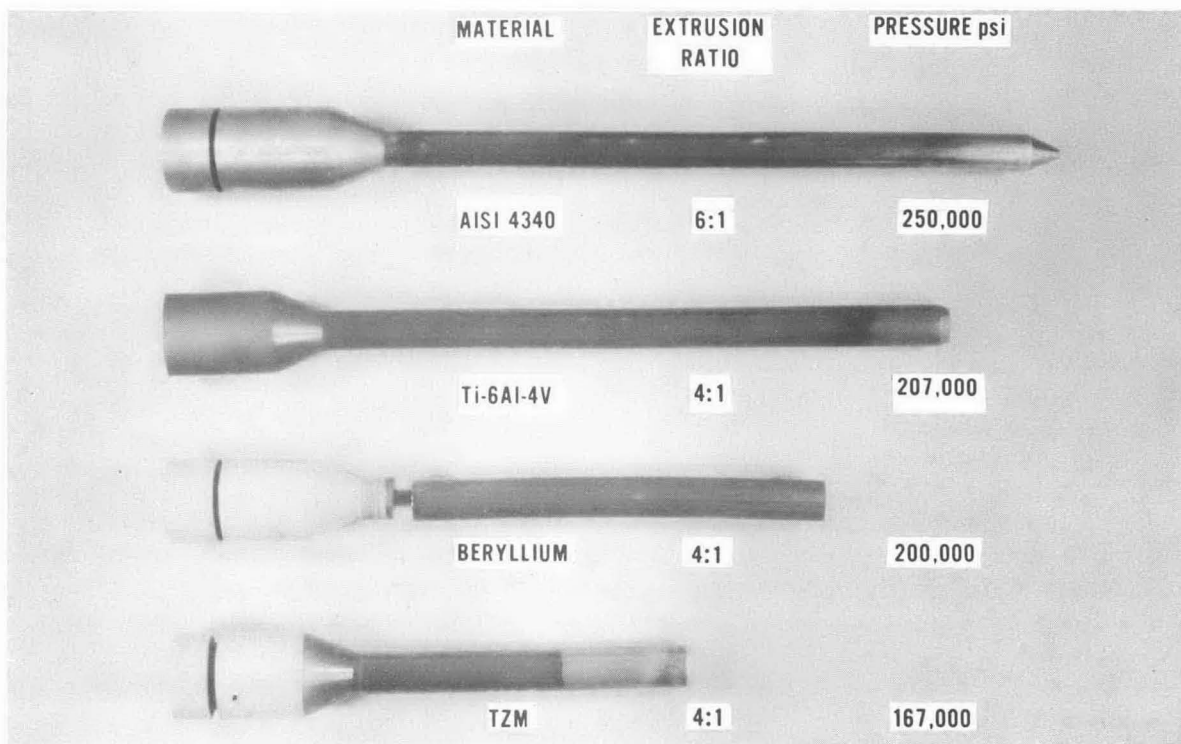
Figures 1 and 2 give examples of hydrostatic extrusions obtained with the range of materials used in this program. The 1100-0 extrusion in Figure 1 was obtained in the previous program⁽¹⁾. In each case, the extrusions represent the maximum extrusion ratios that were attempted in the program. The notable developments made in achieving



39356

FIGURE 1. HYDROSTATIC EXTRUSIONS OF ALUMINUM ALLOYS

7075-0 aluminum billets 1-3/4 inch-diameter.



.39349

FIGURE 2. HYDROSTATIC EXTRUSIONS OF HIGH STRENGTH AND BRITTLE MATERIALS

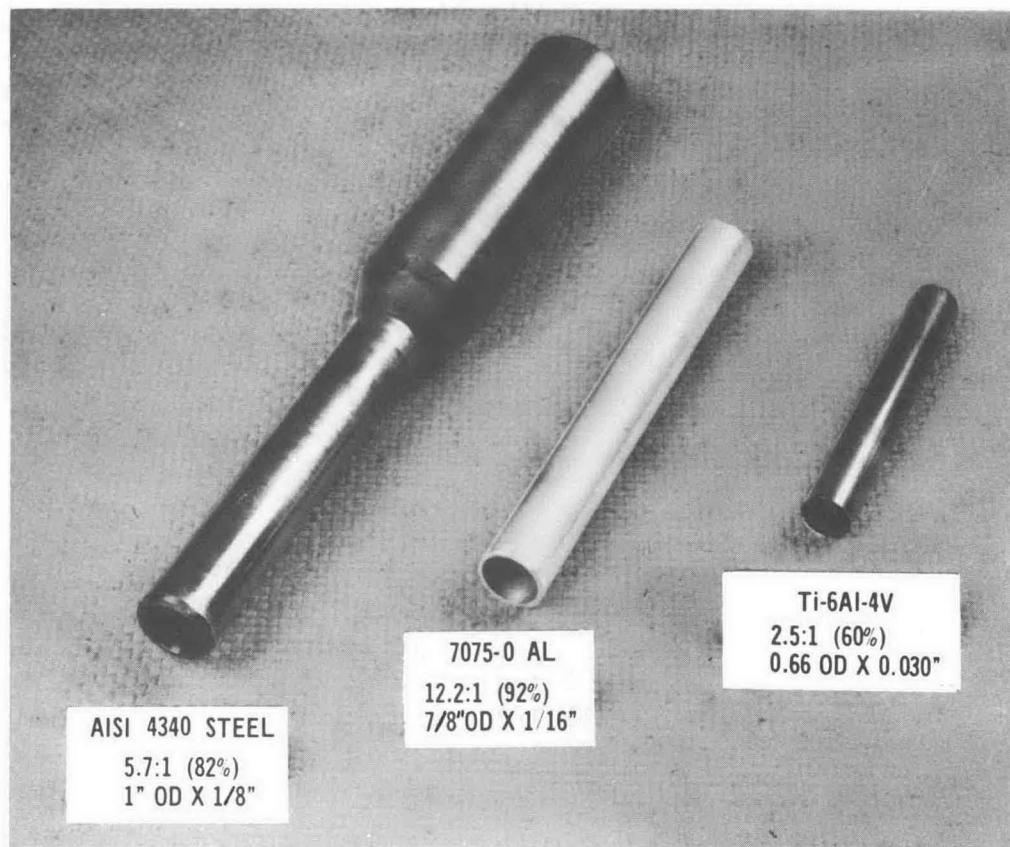
All billet diameters 1-3/4 inches.

these extrusions were in lubrication for the aluminum, steel, and Ti-6Al-4V alloys and in die design for the brittle materials such as beryllium and TZM. Details of these developments are given in Section 1.

Figure 3 shows examples of the tubing produced by hydrostatic extrusion in this program. In the process, the wall thickness of the tube blank was reduced only, the bore remaining essentially constant. The floating-mandrel arrangement used to produce the tubing provided a pressure assistance additional to the fluid pressure. This enabled a capacity for higher ratios with tubing than could be obtained for solid rounds. An analysis for the extrusion of tubing is given in Section 2.

T-sections were produced from round billets and from T-section billets of a variety of materials. Figure 1 shows a T-section extrusion from 7075-0 aluminum round.

Section 2 also describes the hydrostatic extrusion-drawing process, known as HYDRAW, used in this program to produce T-sections and wire. The HYDRAW process was developed at Battelle and the results obtained with the process show considerable promise for its application in a commercial production operation. Whereas in conventional wire drawing, reductions up to about 30 percent are taken per pass (12 percent maximum for beryllium wire), reductions of 50 percent and more were obtained for Ti-6Al-4V alloy, TZM, and beryllium wire. In addition, experiments were conducted in the HYDRAW of T-sections of 7075-0 aluminum. The results showed that problems such as sealing a T-billet in the die could be solved and indicated that finishing of extruded shapes to thin cross sections is another potential application of HYDRAW.



39351

FIGURE 3. HYDROSTATICALLY EXTRUDED TUBING FROM THREE ALLOYS

Data given refers to extrusion ratio, percent reduction, and extruded tube dimensions.

III

EQUIPMENT AND PROCEDURE

Extrusion Tooling

The operational requirements of the hydrostatic extrusion tooling designed and built in the previous program at Battelle⁽¹⁾ were that it withstand internal fluid pressures up to 250,000 psi at temperatures up to 500 F. The extrusion tooling was designed for use in a 700-ton capacity vertical hydraulic press at Battelle. It is shown installed in the press in Figure 4. The general details of the tooling design are shown in the cross-sectional view in Figure 5. The container assembly, consisting of four concentric shrunk-fit rings, is seated on a tapered insert. The extrusion die is located entirely within the bore of the liner and rests directly on the insert.

The columns bolted to the container flange are used to raise and lower the container assembly for inserting and removing the die and billet between extrusion runs. The columns are connected beneath the press platen to a die cushion actuated by an auxiliary double-acting hydraulic system.

The over-all size of the tooling can be judged from the nominal dimensions of the following basic components:

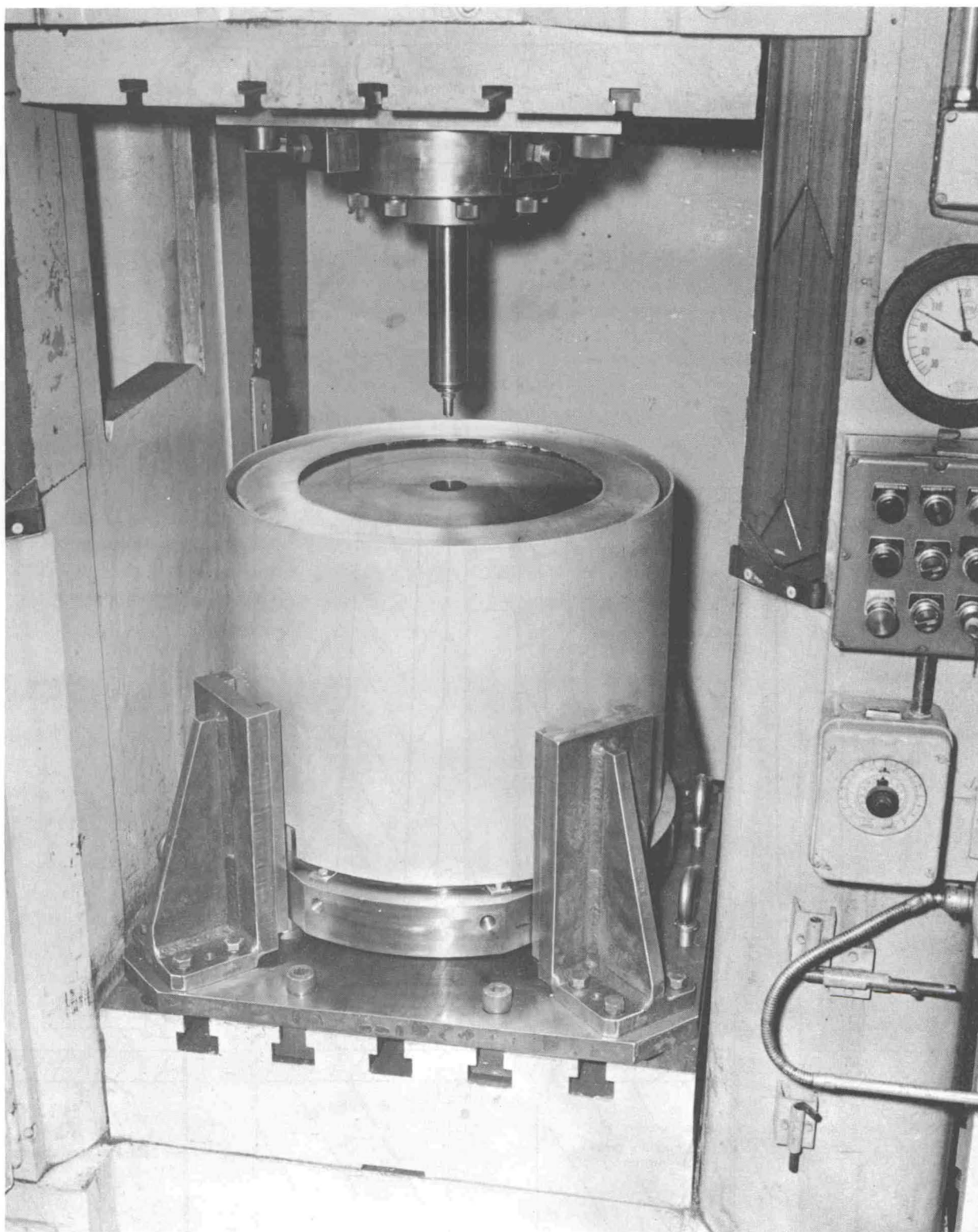
<u>Component</u>	<u>ID, inches</u>	<u>OD, inches</u>	<u>Length, inches</u>
Stem	--	2-3/8	13
Liner	2-3/8	--	20
Container	13-3/8	22	24-7/8

The outside diameter of the container flange is 30-1/4 inches. Billets up to 2-1/4 inches in diameter and 16 inches long can be accommodated within the liner bore.

The design of the container assembly was altered slightly during the course of the program and the details are given in Section 4 of the report along with the complete stress analysis of the tooling and description of the tool materials.

The Hydrostatic Extrusion Operational Sequence

Details of the hydrostatic-extrusion operation are shown in Figure 6. The nose of the billet is tapered to mate precisely with the die-entry surface to prevent fluid leakage. No forcing or wedging of the billet is necessary to obtain a seal. At the start of a typical run, the nose of the billet is dipped into the fluid medium to be used and placed in the die opening. This is done so that the nose will be exposed to the same fluid environment as the rest of the billet. The billet and die are then placed and aligned on the tapered insert as shown in Figure 5. The container assembly is lowered and seated against the tapered insert with a hold-down force to insure alignment and lateral stability. Although a hold-down force of 100 tons (the maximum available on the press) was found to be adequate, it is likely that a much lower force (perhaps in the order of 25 to 50 tons) would



2111

FIGURE 4. HYDROSTATIC-EXTRUSION TOOLING INSTALLED IN 700-TON VERTICAL HYDRAULIC PRESS AT BATTELLE

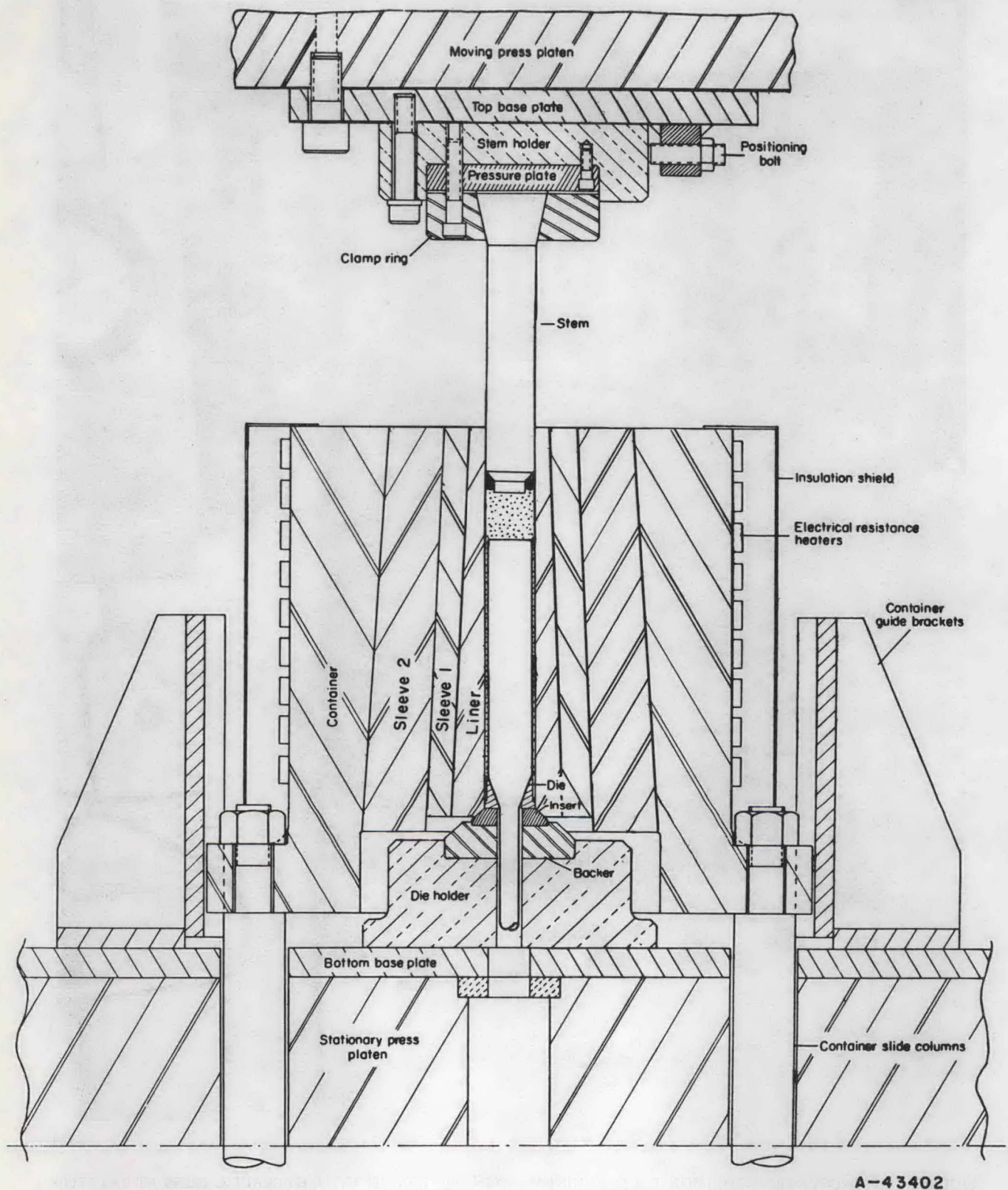


FIGURE 5. ASSEMBLY DRAWING OF TOOLING FOR HYDROSTATIC EXTRUSION

have been sufficient. (It is also possible that the tooling could be designed to eliminate the need for any hold-down force at all.) Next, fluid is added to the liner bore. The stem or ram is forced down against the fluid to build up sufficient pressure to extrude the billet through the die. For long, small-diameter billets for which the die contact area is small, a guide is used on the back end of the billet to prevent it from tilting.

Pressure Control and Measurement

The fluid in the bore of the container was pressurized by axial movement of the stem shown in Figure 5. The stem was secured in a tapered clamp ring which in turn was located in tooling fixed to the top platen of the 700-ton press. Precise axial alignment of the stem with the bore was readily achieved by adjusting screws in the stem-support tooling.

The fluid pressure for room-temperature trials was measured by a manganin coil attached to the bottom of the stem as shown in Figure 6. (A strain-gage transducer described below, was designed for operation at elevated temperatures.) The manganin coil has a resistance of 120 ohms and its resistance change with pressure was calibrated by the vendor to be 1.65×10^{-7} ohm/ohm/psi. A Moseley X-Y plotter (Model 135) is used to measure the resistance change of the "active" coil against a "compensating" manganin coil of 120 ohms at ambient conditions. The recorder produces a chart which shows the fluid pressure against stem travel. An additional check on pressures is given by the stem pressure which is greater than the fluid pressure by an amount proportional to the frictional losses between the stem seal and the container wall. Several measures of stem pressure were available. Two such measures were (1) a load cell between the stem and the pressure plate and (2) a hydraulic-line pressure gage which gives the oil pressure on the main ram of the 700-ton press. Stem pressure from either of these devices was continually recorded on one channel of a 2-channel recorder (Brush Mark 842, Model No. 13-6624-00).

High-Pressure Strain-Gage Transducer

The high-pressure strain-gage transducer described here was conceived for use in measuring fluid pressures in warm hydrostatic extrusion because the manganin gage could not be used much above room temperature. As depicted in Figure 7^(3,4) the temperature coefficient of resistivity of manganin has a zero slope at approximately room temperature, but at higher and lower temperatures the resistivity gradient becomes steep. This leads to considerable errors when the manganin gage is used much above or below room temperature. Also the pressure coefficient of resistivity also changes with temperature and this would introduce still more error.

The strain-gage high-pressure transducer in its final evolved stage is illustrated in Figure 8 along with the shrink-fit bushing and the stem. The operation of this transducer is somewhat similar to one Bridgman⁽⁵⁾ once used. The cap was designed to withstand the external pressure while the strain gages sensed this pressure internally.

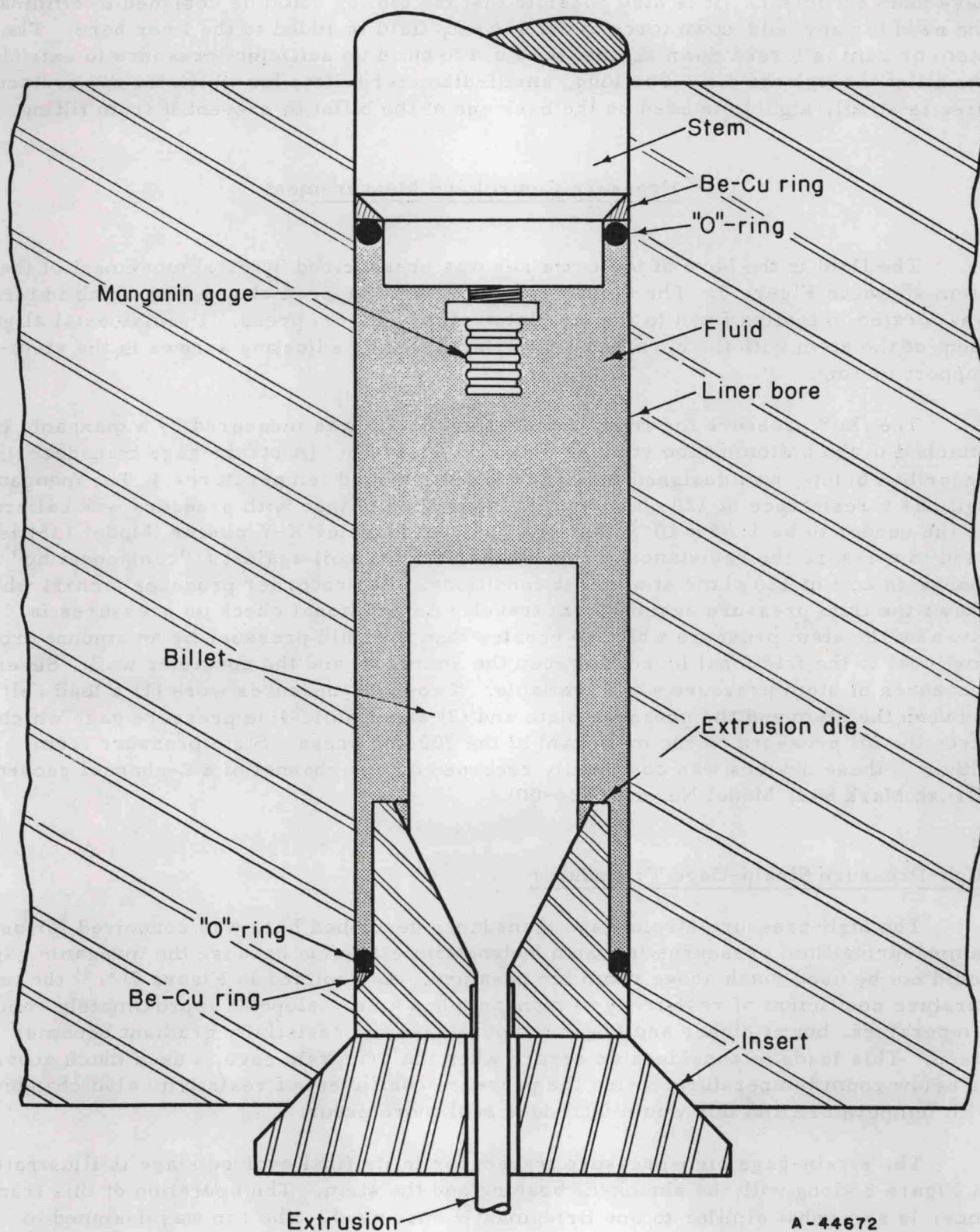


FIGURE 6. DETAILS OF HYDROSTATIC EXTRUSION PROCESS SHOWING THE STEM AND DIE SEAL METHODS, AND PARTIALLY EXTRUDED BILLET

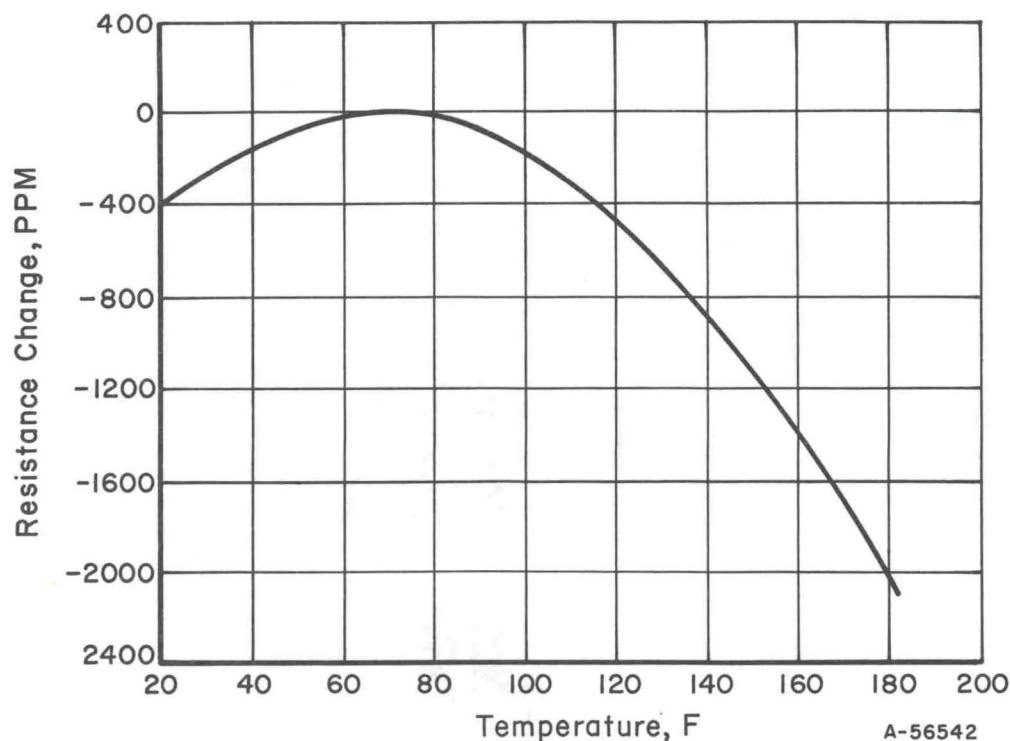


FIGURE 7. TEMPERATURE RESISTIVITY CURVE FOR MANGANIN WIRE

The transducer cap was made of a 6-percent-cobalt grade of tungsten carbide having the following approximate properties:

Specific Gravity	14.9
Hardness	90 R _A
Young's Modulus	80×10^6 psi
Compressive Strength	700×10^3 psi
Tensile Strength	200×10^3 psi
Transverse Rupture Strength	250×10^3 psi
Poisson's Ratio	0.2
Thermal Conductivity	50.0 Btu/hr/ft/F
Thermal Expansion	2.5×10^{-6} in./in./F.

Proportions of the cap were determined in part by the space required to locate the strain gages on the cylindrical bore and also by the design requirement that the maximum compressive stress in the cap should not exceed two thirds of the compressive strength of the material at the operating pressure of 250 ksi. A tight seal between the cap and stem was obtained by lapping the two together. This prevented the high-pressure fluid from leaking from the pressure chamber into the lead wire hole.

A four-arm strain-gage bridge was used in the cap with two "active" and two "temperature-compensating" gages. The two active gages were placed close to the juncture between the cylindrical and the hemispherical bores. The two temperature-compensating gages were placed on a thin wafer of tungsten carbide which in turn was placed in contact with the top of the hemispherical bore. These two gages were stress free. Then the bore was potted with a high-temperature silicon rubber up to depth of the bushing. The bushing which is used to hold the cap on the stem was then shrink

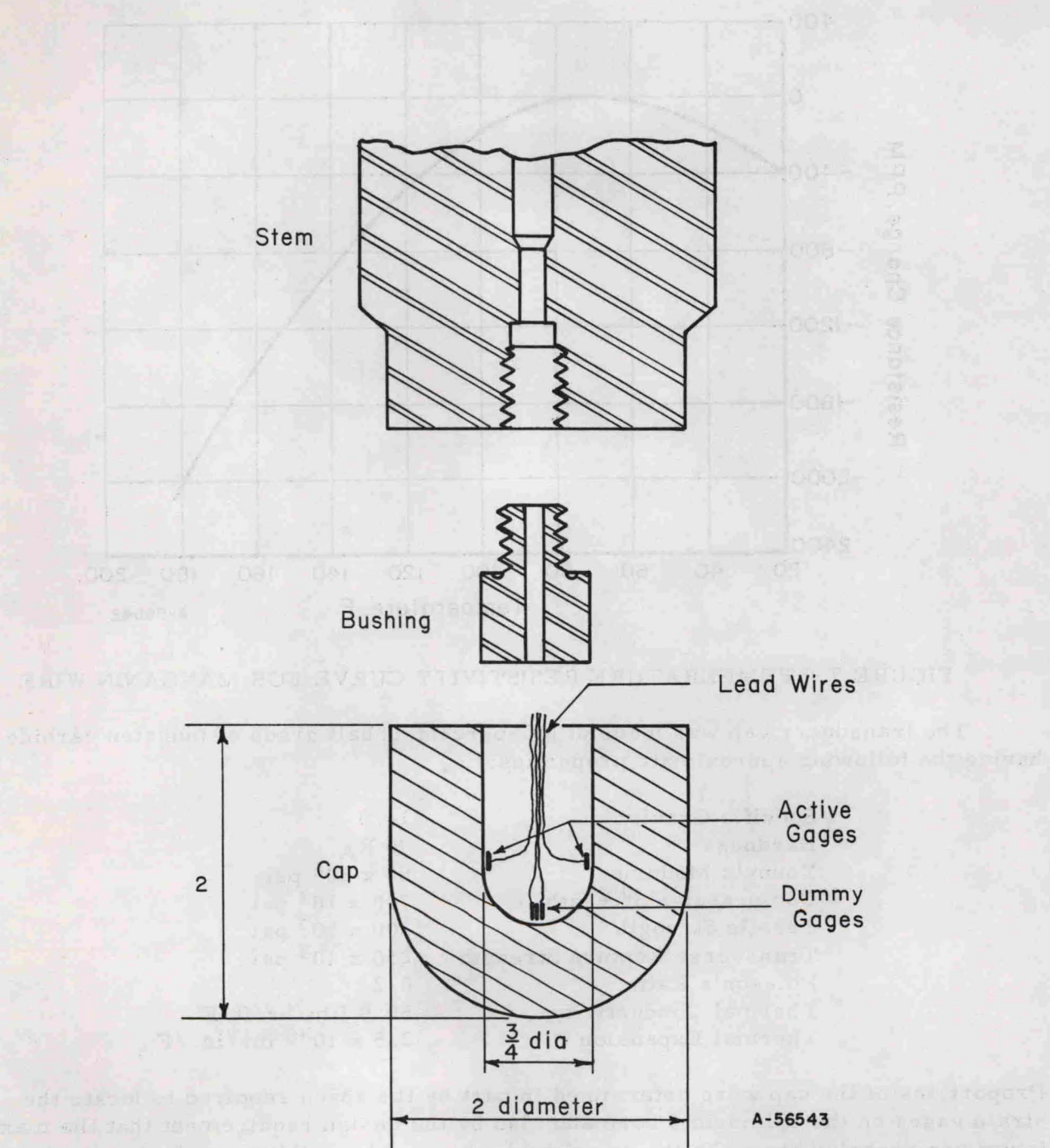


FIGURE 8. HIGH-PRESSURE TRANSDUCER DEVELOPED AT BATTELLE FOR MEASURING HIGH FLUID PRESSURES AT ROOM AND ELEVATED TEMPERATURES

All dimensions given in inches.

fitted into the cup with the bridge lead wires passing through it into the axial bore in the stem. A seal of epoxy adhesive was made where the lead wires leave the bushing to prevent moisture and other foreign substances from entering the cup.

Calibration of the transducer was accomplished by calibrating it against a manganin gage at room temperature in the hydrostatic-extrusion tooling and under the conditions it was to be used. After the initial calibration producing a scaling of 20 microinches/ksi, a one to one correspondence (45 degree plot on an X-Y recorder with both axes scaled in pressure) was obtained between the strain-gage transducer and the manganin gage in further tests. The accuracy and repeatability of calibration was in the order of 1 percent.

The high-pressure transducer performed quite well in many trials at room temperature and at 400-500 F. However, two adverse effects were noted when operating at the elevated temperatures. The first was a slight drift of the instrument zero point while the second was a transient in the zero point of the transducer.

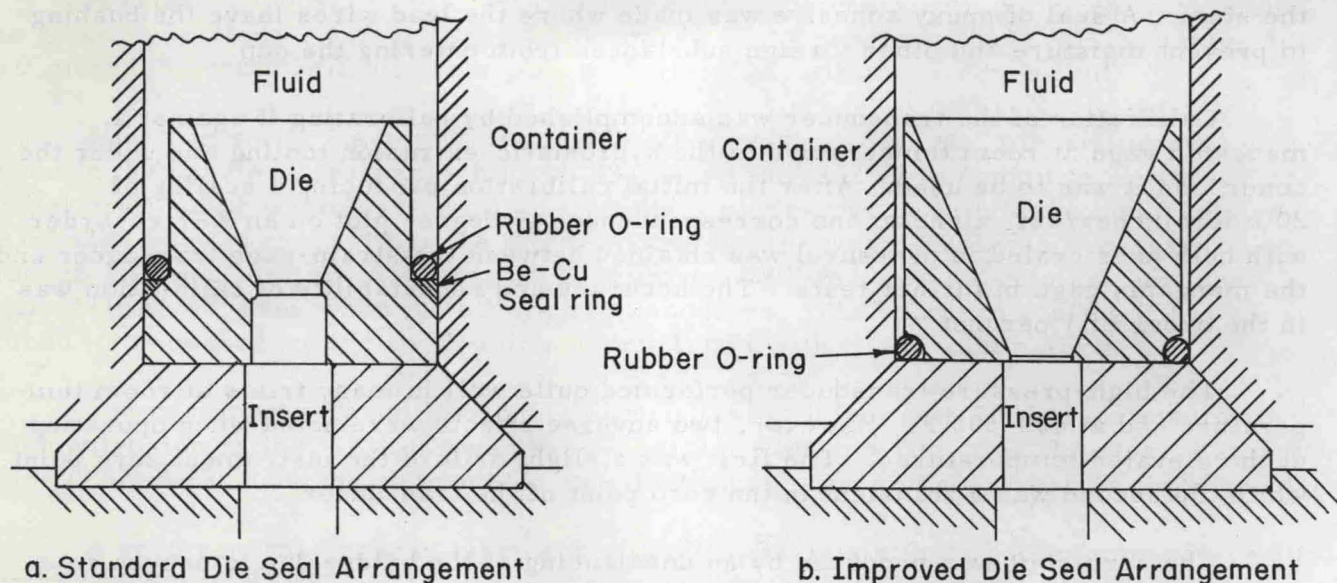
The zero shift was produced by an unbalancing of the bridge due to uneven resistance variations with temperature in each leg either in the strain gages or the connecting lead wires. By soaking the cap in the hot fluid for a few seconds before pressurizing, it was possible to reestablish electrical balance in the strain bridge. Balanced conditions then remained stable throughout the trial. The transient thermal strain which occurred at the zero point, due to the high temperature gradient in the cap, was virtually eliminated by the soaking technique described above.

Toward the end of the experimental trials at 400-500 F, the electrical terminals in the gage failed. In the remaining elevated temperature trials, stem pressure readings were used as a guide to fluid pressures. Gage failure was due to exposure to temperatures above 500 F when the hot fluid burned occasionally. The temperature limitation of the electrical materials used in the transducer was 550 F. For future trials at 500 F, it is recommended that electrical materials capable of higher temperatures than the existing limit of 550 F be used.

Sealing Arrangements

Room Temperature

The sealing method used in the room-temperature trials for the die and stem is illustrated on a die in Figure 9a. This arrangement, used for most of the program, consisted of a beryllium-copper (98Cu-1.8Be-0.2Co) ring of triangular cross section in conjunction with a standard Buna N rubber O-ring. Toward the end of the program, an alternative system of sealing the die was evaluated. This advanced seal arrangement shown in Figure 9b consisted of a single rubber O-ring located at the base of the die. This arrangement is similar in principle to that used at the ASEA High Pressure Laboratory in Sweden. The advancement was essentially an economic one since sealing was never a problem with the previous arrangement. The new arrangement eliminated the need for a metallic seal ring and reduced the die-machining costs somewhat. A major advantage of the improved design is that it allows larger diameter billets to be extruded than with the original design for a given bore size. In the original design, it would have been necessary to have a two-piece die to accommodate large diameters. Sealing with the improved design was achieved in all the trials in which it was evaluated and at pressures up to 250,000 psi



A-56544

FIGURE 9. DIE SEAL ARRANGEMENTS EVALUATED IN HYDROSTATIC EXTRUSION

In view of the very few difficulties encountered with the stem seal design, its use was continued throughout the program. During the program, however, other stem seal designs have been reported such as a U-ring used at ASEA (Robertfors, Sweden) and a rubber O-ring/metal seal ring located in the linear bore as used at Western Electric (Princeton) and ASEA. These designs would be considered for use in future tooling.

Temperature Range of 400-500 F

In the design of a stem to incorporate a high-temperature, high-pressure gage, the stem-seal angle (Figure 10) was increased to 65 degrees from 45 degrees with the design used at room temperature, with the aim of reducing the stem pressure by decreasing the friction between seal and container. The modification was made as a result of the stem-seal experience of Fuchs⁽⁶⁾ with this design. In room-temperature calibration trials, it was found that the stem pressure/fluid pressure difference was reduced by approximately 25 percent when using the 65 degree stem-seal angle.

During the warm trials, three O-ring arrangements were used in the investigation as a result of leakage problems. Three combinations were used:

- (1) A single PTFE O-ring
- (2) A PTFE O-ring plus a Buna-N rubber O-ring
- (3) Two PTFE O-rings.

With the single PTFE O-ring, fluid leaks were frequent. The other two O-ring arrangements successfully contained fluids at pressures up to about 220,000 psi. In none of the arrangements, however, were the rings reusable because of distortion or breakage.

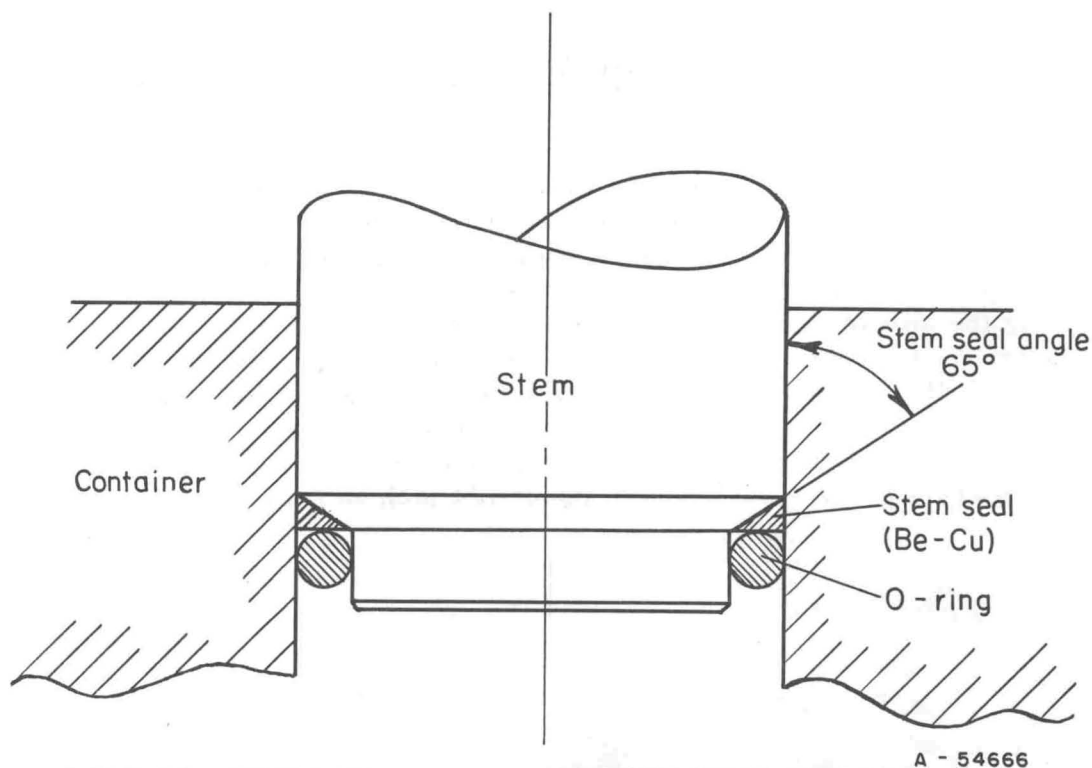


FIGURE 10. STEM-SEAL ARRANGEMENT USED FOR WARM HYDROSTATIC EXTRUSION

In the several trials conducted successfully with a single PTFE O-ring, it was noted that the stem pressure/fluid pressure differences were the lowest of the three combinations. Thus, an increase in stem-seal/container friction occurs with a dual O-ring system. In a single trial, the die seal arrangement shown in Figure 9b was evaluated using a PTFE O-ring. The O-ring expanded on the hot die before the container could be lowered in place, thus preventing sealing. Other O-ring materials however, might be readily used for this application.

Die Design

The die entry-orifice design mainly used in the program was basically as shown in Figure 9. The conical entry was highly polished (in the order of 4μ -inches, CLA) and was, for most trials, maintained at an included angle of 45 degrees. Other die angles were investigated with 7075-0 aluminum and AISI 4340 steel but, at the extrusion ratios achieved and with the lubricants used, were found to require higher extrusion pressures than those required for the 45-degree design. Data for these trials are given in Section 1.

The standard die material was AISI M50 steel heat treated to $R_C 63$. In several trials with two dies, the die entry and bearing surfaces were "Flame-Plated"* with a 0.005-inch-thick coat of tungsten carbide containing 15-17 percent cobalt. The base material of the die was AISI M50 heat treated to a hardness of 55 R_C . The purpose of Flame-Plating was to provide a hard ($R_C 72$), wear-resistant surface which reportedly reduces friction in some applications. Results with these dies reported in Section 1

* Flame-Plate is a proprietary process of the Union Carbide Corporation.

show that the dies had no significant effect on extrusion pressures. Thus, the Flame-Plated die did not appear to reduce friction, but it may be useful for minimizing die wear in a commercial operation.

A further effort was directed toward reducing extrusion pressures by considering the configuration of the entry surface apart from the entry angle itself. The concept that was investigated was the idea of a grooved entry surface. The thought here was that the groove would be occupied by the hydrostatic fluid during extrusion, thereby reducing the amount of billet-die contact area. In this case, the die was "roughened" with a groove to function in a manner similar to a roughened billet which drags fluid in at the die-billet interface. The grooved die evaluated in the program is shown in Figure 11. The groove is about 0.050 inch deep and has a 1/4-inch pitch. The peaks between the grooves are rounded to a 1/8-inch radius. The groove does not intersect the die bearing surface but stops at about 1/4 inch above it.

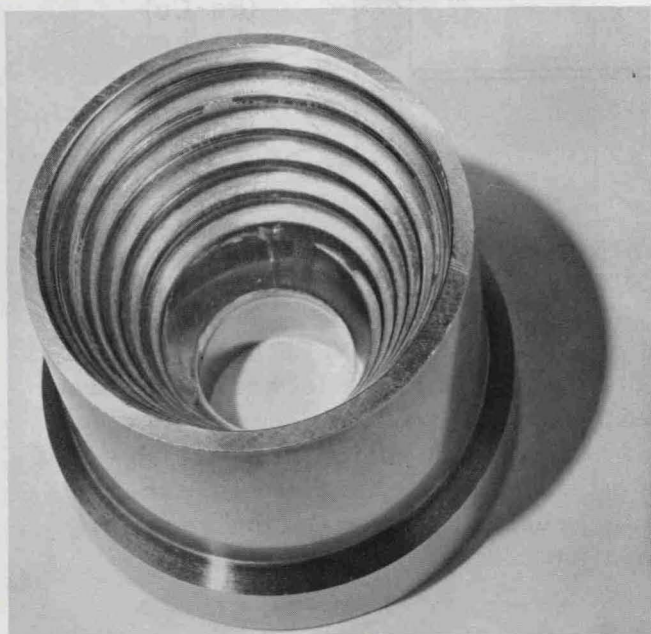


FIGURE 11. DIE DESIGN WITH HELICAL GROOVE IN CONICAL-ENTRY SURFACE

In experiments with the grooved die during extrusion of both AISI 4340 and 7075-0 Al (Trials 284 and 348), the billets were found to have upset into the groove only partially with the steel but completely in the case of the aluminum alloy. This only hindered the extrusion operation because, on continuing extrusion, the billet metal in the grooves tended to shear off rather than flow. This problem might not have occurred if the grooves were much more shallow. At this time, however, it appears that improved lubrication systems and roughening the billet are more effective means of reducing pressures.

On the basis of the results obtained, a die-entry profile of a 45-degree included angle was used as standard for most of the trials with the aim of giving minimum pressure values for all materials. For brittle materials, die design played an important part in obtaining sound products. The evolution of these successful die designs is reported in Section 1. Die design for the extrusion of shapes is described in Section 2.

Billet Materials

For most extrusion trials, the billets were machined, from about 2-inch-diameter bar stock, to 1-3/4 inches in diameter. The extrusion ratio was changed by varying the die-opening size. The billets had noses tapered to the same included angle as the die. The length of the tapered nose was such that the tip was at least flush with the start of the die bearing. The length of the cylindrical portion of the billet was about six inches. The surface finish was in the range of 60-100 microinches, CLA, unless otherwise noted. In some trials, billets less than 1-3/4 inch in diameter were used to achieve a specific extrusion ratio through a die whose orifice area was fixed as in the extrusion of T-sections.

Description of the materials used in this program is given in Table I.

Lubrication

One of the objectives of this program was the development of an efficient lubrication system (billet lubricant plus fluid medium) for each of the materials evaluated. These systems were used later in the program in the hydrostatic extrusion of tubing, wire, and shapes. An efficient system is generally one which will require minimum extrusion pressures and provide an acceptable surface finish. Another factor of importance is the cost of lubrication. However, in this program, efforts were directed mainly towards understanding the mechanics of lubrication so that specifications for efficient lubricants could be laid down.

Factors determining efficient lubrication in hydrostatic extrusion may be divided into four areas:

- (1) The hydrostatic fluid
- (2) Billet lubricants
- (3) Billet conversion coatings
- (4) Billet surface finish.

All of these factors were evaluated. Billet conversion coatings (Item 3) were studied only when the combination of billet lubricant and fluid failed to provide efficient lubrication conditions. This was particularly the case with Ti-6Al-4V alloy. Billet conversion coatings are formed by chemical treatment which change the composition at the surface. Their purpose is to permit lubricants to function more efficiently. The conversion coatings used were tenacious and tended to deform with the lubricant.

In a previous program⁽¹⁾ it was found that, except with some low-strength materials such as 1100-0 Al extruded at low ratios, the fluid alone was inadequate as a lubricant. The effectiveness of a fluid was found to depend upon the base viscosity and the change in viscosity with pressure. Additional lubrication was sought by adding solid film lubricants (MoS₂ or graphite) or oiliness agents directly to the fluid. However, the direct application to the billet of lubricants in the form of a thick film was found to be more efficient and this practice was used in this program.

TABLE I. BILLET MATERIALS USED IN HYDROSTATIC EXTRUSION PROGRAM

Material	Approximate Composition, weight percent	Condition	Source	Properties			
				Ultimate Tensile Strength, 1000 psi	Yield Strength, 0.2% Offset, 1000 psi	Reduction in Area, percent	Elongation, percent
Aluminum	5.5 Zr, 2.5 Mg, 1.5 Cu, 0.3 Cr, balance Al	Annealed	Commercial	33.8	15.5	45.2	23.3
Hardened aluminum	99.999 Al, 6 wt % dispersion of Al ₂ O ₃	80-85 percent theoretical density	Oak Ridge National Lab. (AEC Activity No. 0440-02041)	--	35.0	--	--
Al	0.4 C, 1.75 Ni, 0.80 Cr, 0.25 Mo, 0.75 Mn, 0.25 Si, balance Fe	Mill annealed	Commercial	94.6	55.4	49.0	33.0
Alloy	6.2 Al, 4.2 V, 0.02 C, 0.0009 N, 0.21 Fe, 0.098 O ₂ , balance titanium	Mill annealed	Commercial	143.0	135.0	39.0	21.0
Powder	6.0 Al, 4.0 V, 50 ppm H, 60 ppm N, 1800 ppm O ₂ , 900 ppm Fe, 700 ppm C	90% particles sized between -100 and +325 mesh. Balance -325 mesh	Penn Nuclear Co.	--	--	--	--
tubing	--	Cold drawn and annealed	Wolverine Tube [produced on Contract AF 33(615)-3089]	--	--	--	--
Sections	--	Commercially hot extruded and annealed	The H. M. Harper Co.	--	--	--	--
Molybdenum	0.42 Ti, 0.1 Zr, 0.023 C, Other 0.007, balance molybdenum	Stress-relieved Recrystallized	Climax Molybdenum Co.	107.0 76.0	90.0 50.0	-- 39.0	17.0 38.0
	1.54 BeO, 98.46 Be	Hot pressed block	Brush Beryllium Co.	51.2	36.9	--	2.5
	19.0 Cr, 52 Ni, 5.2 Cb + Ta, 3.0 Mo, 0.9 Ti, 0.8 Al, 0.05 C, 0.35 Mn, 0.35 Si, balance Fe	Hot worked solution- treated	Latrobe Steel Co.	--	--	--	--
	15.0 Cr, 26 Ni, 1.25 Mo, 2.15 Ti, 0.2 Al, 0.3 V, 0.05 C, 1.4 Mn, 0.4 Si, balance Fe	Hot worked solution- treated	Allegheny Ludlum Steel Corp.	--	--	--	--

Cb752 columbium alloy T-section	10.0 W, 2.5 Zr, balance Cb	Hot extruded H-section	E.I. du Pont de Nemours & Co. Inc. [produced under AF 33(657)-11293]	66.0	52.0	--	27.0	--
Ti-6Al-4V wire (0.045-inch diameter)	5.9 Al, 4.0 V, other 0.15, balance Ti	Cold drawn, annealed and pickled	TMCA	140.0	--	--	6.0	--
Beryllium wire (ingot origin 0.020-inch diameter)	0.3 BeO, 0.05 C, 0.07 Fe, 0.12 others, balance Be	Hot drawn, annealed	The Beryllium Corp.	88.0	47.0	--	9.0	--
Beryllium wire (powder origin, 0.020-inch diameter)	2.0 BeO maximum, 0.15 C, 0.18 Fe, 0.36 other, balance Be	Hot drawn, annealed	Brush Beryllium Co.	150.0	137.0	12.4	11.5	--
TZM molybdenum alloy wire (0.1-inch diameter)	0.55 Ti, 0.12 Zr, 0.05 other, balance Mo	Hot drawn, annealed and cleaned	General Electric Co.	125.0	100.0	--	8.0	--

Hydrostatic Fluids

The hydrostatic fluids used in this program for both room-temperature and elevated-temperature trials are described in Table II.

TABLE II. FLUIDS EVALUATED IN HYDROSTATIC-EXTRUSION PROGRAM

Fluid Identification	Description	Kinematic Viscosity, centistokes		Extrusion Temperature, F
		At 100 F	At 500 F	
--	Water	0.76	--	80
--	Castor oil	297	--	80 - 140
--	Ethylene glycol	9.3	--	80
--	Polyethylene glycol	24	--	80
PPE	Mixed isomeric five-ring polyphenyl ether	363	1.2	80 and 500
CBP	Chlorinated biphenyl	44	--	500
TCP	Tricresyl phosphate	35	--	500
TAP	Triaryl phosphate	46	--	500
SE	Silicate ester	6.8	0.88 ^(a)	80 and 400
--	Acidless stearine	Solid	<1	500 - 560

(a) Viscosity at 400 F.

Most of the room-temperature trials were conducted with castor oil as the fluid medium. This fluid was found to have the best combination of efficiency in lubrication and economy in use. Though limited studies showed that water had these qualities too, its corrosive properties might have caused trouble with the experimental tooling. However, a water-based fluid might well prove to be ideal for commercial applications. The ethylene glycol-based fluids performed satisfactory and warrant further investigation as candidate fluids for a commercial operation. The experimental results with this fluid type indicated that compatibility with the billet lubricant was important for efficient lubrication.

A series of fluids listed in Table II was evaluated at 500 F. Because the flash point of silicate ester (SE) was 470 F, trials with this fluid were conducted at 400 F. Of these fluids, polyphenyl ether (PPE) and SE were the most effective with a wide range of materials. Chlorinated biphenyl (CBP) was particularly noxious and did not appear to have commercial potential. Acidless stearine was evaluated late in the program and was used only with beryllium wire. However, the results obtained indicated that this fluid might be as efficient as was PPE and SE with solid rounds. Its main advantage is that it is much cheaper than PPE and SE. Its flash point is about 580 F.

Billet Lubricants

Billet lubricants were most often employed in the form of a wax or lacquer usually containing a solid-film lubricant additive such as MoS₂. More than 50 billet lubricants have been evaluated at Battelle on both this program and in the earlier program⁽¹⁾. For the sake of completeness, all the lubricants evaluated are described in Table III. All the lubricants from L17 and upwards were evaluated in this program. In addition, L8, L9, and L11, which were developed earlier, were further evaluated.

TABLE III. BILLET LUBRICANTS EVALUATED IN HYDROSTATIC EXTRUSION PROGRAM

Lubricant	Source(a)	Description	Lubricant	Source(a)	Description
L1	C	Sodium stearate soap lubricant	L24	B	20 wt% I ₂ in naphthalene
L2	C	Lithium-soap grease containing MoS ₂	L25	B	20 wt% I ₂ and 10 wt% MoS ₂ in naphthalene
L3	B	Silver chloride (solid lubricant) 15.9 wt%	L26	B	20 wt% I ₂ in chlorinated terphenyl (42% chlorine); Arochlor 5442
		30 percent lead naphthenate in oil (E. P. agent)..... 11.9 wt%	L27	B	50 wt% I ₂ in oleic acid
		Calcium-soap grease (base material).. 72.2 wt%	L28	C	20 wt% MoS ₂ in chlorinated paraffin (70% chlorine); Chlorowax
L4	B	Cadmium iodide (solid lubricant)..... 15.9 wt%	L29	C	20 wt% MoS ₂ in chlorofluorocarbon wax, MP 200 F; Kal-F wax
		30 percent lead naphthenate in oil (E. P. agent)..... 11.9 wt%	L30	B + C	Cindol 4616, 50% 4616 castor wax, MP 70 F
		Calcium-soap grease (base material).. 72.2 wt%	L31	C	Fluorocarbon telomer
L5	C	E. P. grease	L32	C	Polyethylene bag
L6	B	30 percent lead naphthenate in oil (E. P. agent)..... 2 wt%	L33	B	55 wt% MoS ₂ and 6 wt% graphite in sodium silicate
		Antimony diamyl dithiocarbamate (E. P. agent)..... 2 wt%	L34	B	50 wt% MoS ₂ in castor wax (more than 20 wt% MoS ₂)
		Dibenzyl disulfide (E. P. agent)..... 2 wt%	L35	B	20 wt% graphite in castor wax
		Ortholeum (commercial E. P. agent).. 2 wt%	L36	B	66 wt% graphite in soda ash paste
		Chlorowax 40 (commercial E. P. agent). 2 wt%	L37	C	Eutectic salt
		Calcium-soap grease (base material)... 90 wt%	L38	C	PTFE lacquer
L7	C	Graphite contained in volatile carrier (aerosol spray)	L39	B	20 wt% I ₂ and 20 wt% MoS ₂ in chlorinated terphenyl (42% chlorine); Arochlor 5442
L8	B	10 wt% graphite in commercial self-drying, semihydrogenated gum resin	L40	C	Fluorosilicone/PTFE; Supermill 125
L9	B	20 wt% MoS ₂ in commercial self-drying, semihydrogenated gum resin	L41	B + C	20 wt% MoS ₂ and Supermill 125
L10	B	50 wt% MoS ₂ in epoxy resin	L42	C	Shell ETR
L11	C	"Castor wax" (hydrogenated castor oil; 158 F m. p.)	L43	B	20 wt% MoS ₂ in Shell ETR
L12	B	5 percent antimony phosphorodithioate in lead dinonylnaphthalene sulfonate..... 5 wt%	L44	B	20 wt% I ₂ in Shell ETR
		Non-soap thickened mineral oil..... 95 wt%	L45	C	Low density polyethylene (0.92g/cc)
L13	C	MoS ₂	L46	B	50 wt% MoS ₂ in low-melting castor wax (Paracin No. 1)
L14	B	10 wt% graphite in castor wax	L47	B	50 wt% MoS ₂ in carbowax 1000 (more than 20 wt% MoS ₂)
L15	C	Chlorinated paraffin (70 percent chlorine)	L48	B + C	L17 lubricant plus metallic lead, copper flake, and graphite (Kopr-Kote)
L16	C	Fluorosilicone fluid thickened with PTFE	L49	B	20 wt% graphite in fluorocarbon telomer
L17	B	20 wt% MoS ₂ in castor wax	L50	B	20 wt% graphite in low-molecular-weight polyethylenes
L18	B	20 wt% PbO in castor wax	L51	C	Metallic lead, copper flake, and graphite (Kopr-Kote)
L19	C	Polyethylene glycol of a waxy consistence, MP 143 F and MW 6000	L52	C	Stearyl stearate
L20	C	L19, but MP 111 F and MW 1540	L53	B + C	Stearyl stearate plus 20 wt% MoS ₂
L21	C	Microcrystalline petroleum wax, MP 180 F	L54	B + C	Stearyl stearate plus 10 wt% graphite and 20 wt% MoS ₂
L22	B	20 wt% MoS ₂ in polyethylene glycol, MW 1000	L55	C	Carbowax 1000 (low-melting-point wax)
L23	B	20 wt% MoS ₂ in low-melting castor oil product	L56	C	Aerosol fluorocarbon with MoS ₂ (Herculon Super)

(a) B = Battelle source, C = commercial source.

A detailed account of the performance of the lubricants with individual materials is given in Sections 1 and 2. During the course of the program, however, a number of efficient lubricants suitable for a wide variety of materials was developed.

Lubricants L11 (castor wax) and L17 (20 weight percent MoS₂ in castor wax) were used in the previous program with AISI 4340 steel but mainly in conjunction with either billet coatings or warm castor oil as the fluid. Further work with these lubricants and AISI 4340 showed that neither the billet coating nor the warm fluid was necessary though L11 was less efficient than L17. Lubricant 17 was also an efficient lubricant with Ti-6Al-4V alloy when the billets were anodized. The anodized coating (C5) was found to be necessary for room-temperature trials with this titanium alloy.

The castor wax-based lubricants were not so efficient with 7075-0 aluminum at high extrusion ratios. A improved base lubricant with this alloy was the stearyl stearate type (L52, L53, L54) which provided excellent lubrication and good surface finishes.

A good general-purpose lubricant with all materials at both room temperature and up to 500 F was PTFE. This lubricant was used with all the difficult-to-work materials such as the superalloys and brittle materials and only in a few cases did the lubricant partially break down. However, this lubricant is relatively expensive to apply, troublesome to remove (by heating to 600 F where PTFE is toxic), and may be too expensive to use commercially except for extrusion of the more exotic materials.

A wide range of lubricants was found to be effective at 500 F with AISI 4340 steel but the selection of good lubricants for Ti-6Al-4V alloy at this temperature was more limited. The best candidate billet lubricant for further evaluation was L33 (55 weight percent MoS₂ and 6 weight percent graphite in sodium silicate) which was easily applied and removed. Lubricants having a sodium silicate base show considerable promise for warm hydrostatic extrusion.

It is worthy of note, that the techniques required for applying these billet lubricants were important. In the case of the waxes and stearyl stearate, there appeared to be a minimum thickness of the solid film below which lubrication breakdown occurred. It was found that if the lubricant flaked off at the conical billet nose due to careless handling, then the billet would either seize in the die or the product would be badly scored in the area where flaking occurred. To ensure a good "bond" between the lubricant film and the billet surface and to prevent excessive film thickness, it was found necessary to heat the billets before lubricant application rather than apply the melted lubricant to the cold billet.

Billet Conversion Coatings

Billet conversion coatings were evaluated with AISI 4340 steel and Ti-6Al-4V alloy. The investigation of coatings on steel billets was a carry-over from the previous program⁽¹⁾ where conventional cold forging lubrication was used in the initial studies in hydrostatic extrusion. Coating C1, which is described with the other coatings evaluated in this program in Table IV, was not found to be necessary on steel but it always provided marginally lower pressure requirements than when it was not used. Coatings C3 and C4 were not as effective as C1.

TABLE IV. BILLET CONVERSION COATINGS EVALUATED IN THE
HYDROSTATIC-EXTRUSION PROGRAM

Coating	Source	Description	Billet Material Treated
C1	Commercial	Zinc phosphate coating	AISI 4340
C2	Battelle	Fluoride-phosphate coating	Ti-6Al-4V
C3	Battelle	Metal-free phthalocyanine	AISI 4340
C4	Battelle	Lead coating	AISI 4340
C5(a)	Watervliet	Anodized coating	Ti-6Al-4V
	Arsenal		
C6(a)	Battelle	Diffused nickel-plating	Ti-6Al-4V

(a) C5 and C6 were numbered in the Interim Reports as C3 and C4, respectively, in error. However, duplication of coating numbers did not occur in the individual reports.

As a contrast, however, Coating C5 was always necessary in the cold hydrostatic extrusion of Ti-6Al-4V alloy at room temperature. Without C5, severe lubrication breakdown occurred often and resulted in a poor quality product. However, at 500 F, it was not necessary to use coatings with this alloy; excellent lubrication was obtained with billet lubricant (L33) alone.

IV

CHARACTERISTICS OF PRESSURE-DISPLACEMENT CURVES

The effectiveness of lubrication systems in hydrostatic extrusion is evaluated by comparing extrusion pressures, extruded surface finishes, and the general characteristics of the pressure-ram displacement curves produced during extrusion. The pressure-curve characteristics were found to differ considerably for different lubricant systems and billet materials.

It has been found that the extrusion pressure-displacement curves can be classified into families as shown in Figure 26. That figure is placed at the end of the text in Section 1 on a foldout page for ready reference when the extrusion data are being examined. Each family of curves is designated by a letter, and the number following it classifies the typical runout characteristics within each family.

Curves Types A, B, C, and D represent quality of lubrication in decreasing order of effectiveness. These curve types have been numerically classified further according to the following characteristics during runout:

<u>Number</u>	<u>General Runout Characteristics</u>
1	Constant
2	Decreasing
3	Increasing
4	Special

Type A Curves. One of the aims of the experiments on lubrication systems in the program was to obtain conditions giving a curve of Type A 1 which represents completely effective lubrication throughout the extrusion stroke. Experience has shown that once this type of curve is achieved, for a given material and extrusion ratio, other lubrication systems may not lower the value of P_r (runout pressure) markedly and therefore the curve very likely represents near-optimum lubrication conditions. There is no breakthrough pressure (P_b) peak above the runout pressure which suggests that the static friction, μ_s , is about the same as the kinetic friction coefficient, μ_k , developed once the billet starts to move.

The runout characteristics in the other Type A curves may represent partial lubrication breakdown due to pressure-temperature effects at the billet-die interface or changes in flow strength due to adiabatic heating of the billet.

Type B Curves. All the curves in this category are generally characterized by a rounded breakthrough pressure peak (P_b) followed by a smooth runout curve at a lower pressure (P_r). The occurrence of a rounded pressure peak has been attributed to the fact that μ_s is somewhat higher than $\mu_k^{(1)}$, but not sufficiently to cause a sharp stick-slip peak. In some cases, the breakthrough pressure peak is sharp, indicating a stick-slip situation at breakthrough only.

Type C Curves. These curves are similar to Type B curves except that one or a few cycles of stick-slip follow the breakthrough pressure peak. Here stick-slip is generally not severe, its amplitude decreasing to give a smooth runout curve.

Stick-slip by hydrostatic extrusion is caused by the energy stored in the fluid at P_b being sufficient to overcome μ_s but much more than necessary for μ_k . Consequently extrusion occurs very rapidly and is accompanied by a sharp drop in pressure⁽¹⁾. The μ_s achieved at the P_r level apparently is not sufficiently greater than μ_k to cause stick-slip of the same magnitude to occur again.

Type D Curves. In these curves stick-slip is generally severe and continues throughout the stroke. Extrusion takes place at extremely rapid rates after each pressurizing stroke. The lower pressure level reached after each "slip" tends to occur at the same level during each cycle of stick-slip. Experimental results have indicated that this level represents fairly well the value of P_r if stick-slip had not occurred. For this reason, the level is designated as " P_r " to indicate that this is the apparent runout pressure. Often the amplitude of stick-slip ($P_b - P_r$) is about 30 percent greater than " P_r ".

It is of interest to note that, because of the decreasing stick-slip in Curve D 2, a smooth runout might eventually be obtained if extrusion were continued further. In Curve D 3, a constant amplitude of stick-slip is superimposed on an increasing " P_r ". As a contrast, however, the amplitude of stick-slip has also been observed to increase over an apparently constant " P_r " value as in Curve D 4.

ASSESSMENT OF FLUID HEATING EFFECTS DURING COMPRESSION

A study was made to determine the temperature change that occurs in the hydrostatic fluid during compression to various pressure levels at various stem speeds. Such information is of value in evaluation of lubrication systems and in precision calibration of the manganin gage used in measuring fluid pressure.

The faster the stem speed, the greater the amount of adiabatic heating of the fluid due to compression. If the fluid temperature reached just prior to extrusion is too high, the lubrication system may break down. Thus, it may be necessary to alter the lubrication system to suit the stem speed as well as the pressure level for optimum operation.

It was also considered important to determine the extent to which fluid temperature might influence the calibration of fluid-pressure readings as measured by the manganin gage. If the active manganin coil in the fluid is at a temperature much different than that of the compensating coil exposed to ambient temperature and pressure, an error may be introduced in the fluid-pressure measurements. The size of the error depends on the temperature difference. For example, if the active coil were at 120 F, calculations indicate that the pressure readings would be about 3000 psi low. The significance of this error, of course, depends on the pressure level during extrusion. (The error would be 3 per cent at 100,000 psi, 1.5 per cent at 200,000 psi, etc. The higher the pressure level, the less significant the error becomes.)

Of course, the temperature that the active coil attained during compression of the fluid would depend on the heat-transfer time available. Since the coil used in the program was encapsulated in a fluid-filled metal bellows, the heat transfer time would be appreciable. Furthermore, although faster stem speeds mean higher fluid temperatures, they simultaneously reduce the time available for heat transfer prior to and during extrusion. In reality, then, fluid-pressure measurements made at relatively fast stem speeds may not be very much in error. However, this was still conjecture, and it remained to determine for certain what, in fact, the quantitative effects of stem speed and pressure level are on fluid-temperature and -pressure measurements. Thus, it was considered worthwhile to undertake such a study.

Measurements of fluid-temperature fluctuations during compression were made with a Chromel-Alumel thermocouple sealed in a plug. The plug was made the same size and shape as a standard billet (1-3/4 inches in diameter x 6 inches long x 45-degree tapered nose) to simulate the heat sink provided by the billet prior to extrusion. The plug was inserted in a standard hydrostatic extrusion die to seal off the fluid. To prevent unintentional extrusion, the plug was hardened to R_C 60.

Temperature fluctuations in castor oil were measured during compression to pressures (nominal) of 100,000 psi, 200,000 psi, and 250,000 psi. Stem speeds were to be evaluated at each pressure level. The experimental data for a stem speed of 1 ipm are given below.

Trial	Fluid Pressure, psi	Time, minutes		Fluid Temperature, F	Temperature Change, F
		To Reach Pressure	Held at Pressure		
1	0	0	0	73	
	112,000	2.17	0	123	+50
	112,000	--	5.0	110	-13
2	0	0	0	~50 ^(a)	
	210,000	3.25	0	141	~+90
	210,000	--	4.75	132	-9
3	0	0	0	52 ^(a)	
	246,000	3.75	0	155	+103
	246,000	--	2.75	144	-11

(a) The fluid cooled to below room temperature on decompression from the previous trials.

It is noted that small, but appreciable, increase in fluid temperature occurred even at the relatively slow stem speed of 1 ipm. It is of interest also that the temperature dropped while holding at pressure were relatively small (9 to 13 F), considering the large heat sinks available in the container assembly and the billet-shaped plug, both of which were at room temperature. Of particular importance was that no significant drop in fluid pressure readings was noted during holding at 112,000 or 210,000 psi, suggesting that no appreciable temperature change occurred in the active coil.

It was during the trial at 246,000 psi that a liner failure occurred after holding at this pressure for 2-3/4 minutes. No data on pressure fluctuations during the holding period were obtained.

The trials were not continued at higher stem speeds in the repaired container because sufficient data was obtained from the above trials. It was felt that if fluid pressures were unaffected by a 90 F change in temperature over a holding period of up to 5 minutes, then at higher stem speeds, pressures would not be affected by even higher possible fluid temperatures because of the short time interval during extrusion.